

論文94-31B-6-4

레이돈 변환 방식을 이용한 비행 물체의 3차원 위치 추정

(3-D Location Estimation of Airborne Targets Using a Modified Radon Transform)

崔在虎*, 郭勳星*

(Jae Ho Choi and Hoon Sung Kwak)

要約

적외선 연속 영상들 속에서 확인하기 힘든 작은 비행 물체의 탐지와 그 물체의 궤적의 3차원 위치를 추적하기 위하여 레이돈 변환으로 부터 도출한 새로운 투사 방법을 제안한다. 화소당 SNR이 매우 낮고 영상에 나타난 비행 물체의 크기가 화소보다 작기 때문에 비행 물체의 궤적을 추적하기 위해서는 여러 개의 영상프레임을 적재해야 한다. 3차원 연속 영상 데이터(시간 연속 프레임)는 3차원 레이돈 변환을 이용하여 임의의 방향에 따라 2차원의 여러 표현 방식들로 구성 시킬 수 있기 때문에 우리의 투사 변환 방법은 3차원적 문제를 2차원의 투사 공간에서 분석 가능케 한다. 제시된 방법은 3차원 데이터 전체를 그대로 분석 처리하는 계산 부담을 크게 덜어 줄 뿐만 아니라 낮은 SNR 값에서 얻어진 실험 결과 또한 3차원 비행 물체 궤적의 확실한 탐색과 추정을 보여준다.

Abstract

A new projection-based approach derived from the Radon transform for detecting and estimating 3-D locations of unresolved targets in a time-sequential set of infrared imageries is presented. Since the signal-to-noise ratio per pixel is very low (a dim target) and target is unresolved (of spatial extent less than a pixel), one must rely on integration over target tracks which span over many image frames. Since the 3-D volume of spatio-temporal data(time-sequence frames) can be decomposed into 2-D multiple representations along arbitrary orientations utilizing the 3-D Radon transform, our projection-based transform method enables us to analyze the 3-D problem in terms of its 2-D projections. Our method not only alleviates the great computational expense of processing entire set of images as a whole, but the results reveal that the proposed strategy produces a robust detection and estimation of the 3-D target trajectories even at low SNRs.

I. Introduction

* 正會員, 全北大學校 컴퓨터工學科
(Dept of Computer Engineering Chonbuk Nat'l Univ.)
接受日字 : 1993年 9月 7日

Remote sensing of small moving targets in a time-sequential set of digital image data is a problem that has received much attention

in recent years. Examples include ground-based sensing of satellites, meteors, and asteroids and detection of airborne targets such as aircrafts in satellite acquired imagery [1,2,3]. This paper is directed toward the last example, tracking a small, dim moving target in the three-dimensional (two spatial and one temporal) space. Image data acquired using a focal plane array of infrared or optical sensors is often used. The sensor array collects a time-sequential set of two-dimensional image frames, each of which contains background clutter, noise from the electronics, and targets, if present. Although the target size varies depending on the actual target size, the satellite platform altitude, the target speed, and the optics, of particular interest in this work is targets whose size is on the order of one pixel. A target, if present, usually moves in a direction approximately perpendicular to the sensor line-of-sight (so its size is constant) and moves through the field of view while the background stays relatively constant. If a target is in the field of view, it appears in a succession of frames as it moves. Detecting such targets in a sequence of noise images is challenging since the signal-to-noise ratio per pixel is very low (a dim target) and the target is unresolved (of spatial extent less than a pixel). In addition, since there is a large amount of uncertainty as to the pattern and location of target tracks, good algorithms must consider a large number of possibilities.

Recently, the research efforts have proposed the solutions to the problem of detecting dim, unresolved target tracks. First, a Hough transform-based algorithm for extracting the target tracks was developed [4]. The results show that this algorithm performs well under variety of conditions, but as the SNR is reduced significantly the performance degrades rapidly. Later, extending this algorithm, the modified Hough transform-based algorithm was

proposed to detect linear and curved tracks [5]. On the other hand, the track detection problem was reformulated as the two-hypothesis detection theory problem. This provides alternative methods for evaluating algorithm performance in terms of probability of detection, probability of false alarm, and a posteriori probabilities [6]. Each of these algorithms has been evaluated using sets of 2-D track map sequences. A track map sequence results from projecting a preprocessed time sequences of image frames onto one 2-D track map image. The track map data may still contain some noise; however, it is assumed that the remaining noise is white.

There is a limitation, however, in overall performance when using the temporal projection to create a 2-D track map sequence from the original 3-D (space and time) image data, especially when the targets are dim. Even if projection is performed optimally, it causes a significant reduction in the effective SNR as compared to the SNR of the original 3-D data [7,13]. In this paper, we propose a solution circumventing this problem by using the Radon transform. In general, the Radon transform produces a set of (N-1)-dimensional projections from an N-dimensional function. Although there is an increase in the number of computations needed to compute the projections at arbitrary orientations there is also an increase in detection and estimation ability of target tracks by successfully incorporating all available knowledge overestimated in the set of projections, which also contains the temporal projection as an element. Since the 3-D volume of spatio-temporal data (time-sequence frames) can be decomposed into 2-D multiple representations along arbitrary orientations utilizing the Radon transform, the presented projection-based transformation method analyzes the 3-D problem in terms of its 2-D projections. This method, moreover, has an advantage of alleviating the greater

computational expense of processing entire set of images as a whole.

II. New Approach

Introduced early in twentieth century [8], the Radon transform theory has demonstrated its usefulness in applications for pattern recognition, and feature extraction [9]; and nuclear medicine and imaging by magnetic resonance [10]. Fundamental to most of these applications is that the Radon transform enables feature extraction and classification at high speed by converting N-dimensional computation in a sequence of (N-1)-dimensional operation [11]. As done in the Radon transform, our approach to estimating the locations of unresolved target trajectories in a 3-D volume of images is to take a number of different projections at arbitrary orientations.

In this paper the special cases of two- and three-dimensional Euclidean (or image) space are considered. Consider, for example, a two-dimensional general function $G(x,y)$. Computing the Radon transform consists of computing the projections of an image along a particular pattern, e.g., a straight line (the so called ray)

$$\kappa = y \cos \phi - x \sin \phi \quad (1)$$

and the integral of $G(x,y)$ along a ray is called ray integral and a set of ray integrals forms a *projection*

$$R(\kappa; \phi) = \int_{-\infty}^{\infty} G(x,y) d^2r = \int_{-\infty}^{\infty} \int_{-\infty}^{\infty} G(x,y) \delta(\kappa - y \cos \phi - x \sin \phi) dx dy \quad (2)$$

$R(\kappa; \phi)$ as a function of κ is the parallel projection of $G(x,y)$ for angle ϕ . The entire two-dimensional distribution $R(\kappa; \phi)$ taken along a set of parallel rays defined by the Dirac-delta function is referred to as the Radon transform of $G(x,y)$.

Similar to the 2-D Radon transform, a general 3-D function $G(x)$, i.e. $x \equiv [x,y,$

$z]$, can be decomposed into a set of 2-D projection planes that are parameterized by an arbitrary two-component vector. Mathematically, the 3-D Radon transform can be written as

$$R(\kappa; n) = \int_{-\infty}^{\infty} \int_{-\infty}^{\infty} \int_{-\infty}^{\infty} G(x) \delta(\kappa - x \cdot n) d^3x \quad (3)$$

For a three-dimensional volume (or object) $G(x)$, $R(\kappa; n)$ denotes the surface integral of $G(x)$ over the plane $\kappa = x \cdot n$ where $n \equiv [n_1, n_2, n_3]$ denotes a unit vector normal to the plane and κ is the distance of the plane from the origin. The Radon problem is to determine $G(x)$ given the set of integrals $R(\kappa; n)$ for all κ and n . To recover the complete body, the areas of all possible cross sections of body are needed. However, Lewis [12] has shown that more restricted information could be used to achieve complete or partial recovery.

In our generalized projection algorithm based on the 3-D Radon transform, however, the Radon transform is modified into a simpler form utilizing the symmetry and aligning the aspects of projection. Moreover, instead of using the surface integration defined in Eq. (3), the maximum value projection scheme [13] is incorporated in the implementation. As shown in Figure 1, our modified Radon transform of a time-sequential 3-D volume of image data that contains possible target tracks can be written as follows:

$$P_m(\kappa_\phi, \tau) = F_t [T(x,y,t)] = \text{Max}_{t=0}^{N-1} [T(x,y,t) \delta(\kappa_\phi - y \cos \phi + x \sin \phi)] \quad (4)$$

where $\kappa_\phi = y \cos \phi - x \sin \phi$ represents the function for the ray and $T(x,y,t)$ is the target trajectory function. $P_m(\kappa_\phi, \tau)$ denotes a set of parallel projections taken along a series of parallel projection planes defined by the Dirac-delta function. The entire three-dimensional distribution $P_m(\kappa_\phi, \tau)$ as a function of κ_ϕ and τ for a given value of ϕ is the proposed modified Radon transform of

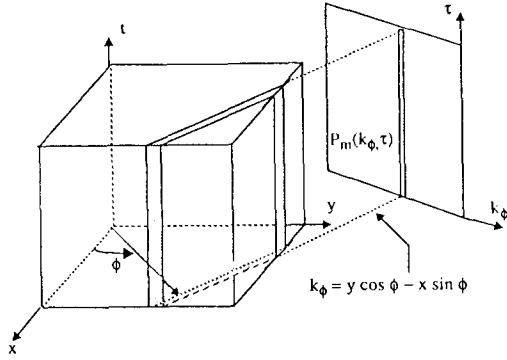


Fig. 1. Geometry for the modified three-dimensional Radon transform.

$T(x, y, t)$. We refer the entire distribution as the parallel projections of $T(x, y, t)$. As a note, $F_{\phi} [\]$ denotes the simplified notation of Eq.(4) that represents the forward transformation along the projection angle .

Since the number of projections is arbitrary, we have taken another parallel projection set other than the one obtained by Eq.(4). By changing the aspect of projecting plane as

$$\kappa_{\gamma} = t \cos \gamma - y \sin \gamma \quad (5)$$

the second set of parallel projections can be obtained as follows:

$$P_m(\kappa_{\gamma}, \nu) = F_{\gamma}[T(x, y, t)] = \text{Max}_{x, y, t} [T(x, y, t) \delta(\kappa_{\gamma} - t \cos \gamma + y \sin \gamma)] \quad (6)$$

For each of two projection sets, the number of projections is arbitrary and not limited to a certain quantity. Since that quantity is the parameter that is to be determined, we take variables C_{ϕ} and C_{γ} for representing the number of projections in each set, respectively. In other words, by controlling these two parameters the total number of projections taken is determined. Once all the parallel projections are obtained, the target track parameters for each one of the projection frames are estimated by using the 2-D Hough transform. The straight line in a

Cartesian coordinate (image space) system can be parameterized in several ways depending on a specific application. In this paper, we have used the normal parameterization as follows:

$$\rho_x = x_x \cos \theta_x + y_x \sin \theta_x \quad (7)$$

where ρ_x is the normal distance from the line to the origin of a projection image space indexed by x_x and y_x , and θ_x is the angle of the normal line with respect to the x_x -axis. Eq.(7) defines a transformation from the projection image space to the Hough parameter space in which the coordinate axes are indexed by the Hough space parameters ρ_x and θ_x .

In the last stage, an estimate of the 3-D target trajectory in the original 3-D image space is then obtained by back-projecting two-dimensional estimates, i.e., (ρ_i, θ_x) for $i=0, 1, \dots, C_{\phi}-1$ and $(\rho_j, \theta_{\gamma})$, $j=0, 1, \dots, C_{\gamma}-1$, obtained by 2-D Hough transform for each one of projections. The backward projection for reconstruction, as shown in Figure 2, is expressed as follows:

$$T'(x, y, t) = \sum_{i=0}^{C_{\phi}-1} F_{\phi}^{-1}[T_i(\kappa_{\phi}, \tau)] + \sum_{j=0}^{C_{\gamma}-1} F_{\gamma}^{-1}[T_j(\kappa_{\gamma}, \nu)] \quad (8)$$

where $T_i'(\kappa_{\phi}, \tau)$ and $T_j'(\kappa_{\gamma}, \nu)$ are the estimated two-dimensional target track functions obtained by the 2-D inverse Hough transform for each one of the projection frames

$$T_i(\kappa_{\phi}, \tau) = \rho_i' - \kappa_{\phi} \cos \theta_i' - \tau \sin \theta_i' = 0, \forall i \quad (9)$$

$$T_j(\kappa_{\gamma}, \nu) = \rho_j' - \kappa_{\gamma} \cos \theta_j' - \nu \sin \theta_j' = 0, \forall j \quad (10)$$

$T'(x, y, t)$, after thresholding, is the reconstructed three-dimensional target trajectory function. The convergence of three-dimensional track estimation from the set of projection data is limited by the input image frame signal-to-noise ratio and the discretization errors(data sampling and quantization).

Discretization errors occur when the data is recorded discretely and when there is a projection onto a plane that is not parallel to one of the spatial or temporal planes.

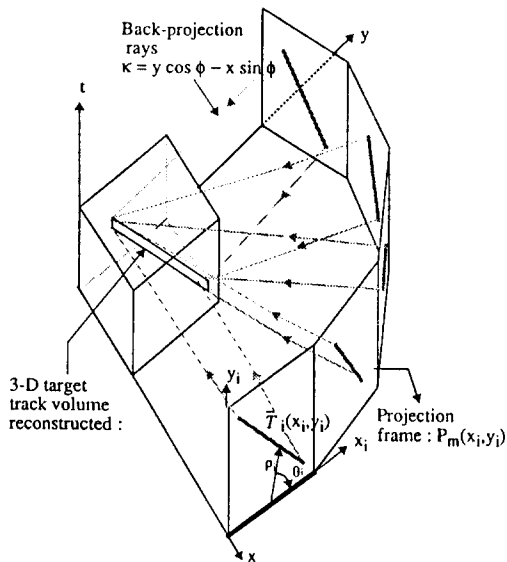


Fig. 2. 3-D estimated track reconstruction using backward projection.

III. Simulations

Simulations were run to demonstrate the performance of our projection-based transformation method for estimating tracks of unresolved targets. The primary target track geometry is a non-maneuvering straight lines. The objective is to study the behavior of our algorithm as a function of the number of projections, the signal-to-noise ratio, the number of image frames. As shown in Figure 3, two sets of real infrared data provided by the Naval Research Laboratory (NRL) referred to as HiCamps were used. Each data set has a frame size of 32×32 pixels and up to 46 frames in the temporal direction to accommodate the longest possible track of a target moving at a speed of one pixel per frame. Since an image sequence with a real target was not available, the targets were also synthetically generated and superimposed

into the time-sequential set of infrared data with a variable amount of white Gaussian noise.

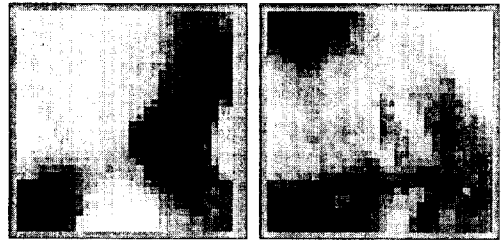


Fig. 3. The real infrared images: the HiCamp I (left) and II (right).

The simulation results showed us a highly robust parameter estimation performance of our algorithm by yielding a target tracking ability down to 3.5 dB in a 2-D Hough parameter estimation of moving target tracks. A typical simulation results are shown in Table 1. The algorithm was tested in terms of the number of projection (PROJ), number of image frames in the time-sequence data (FRM), and the signal-to-noise ratios in decibels. The pair of numbers in the parentheses represents the estimated 2-D Hough parameters given the true trajectory parameters at $\rho = 18$ and $\theta = 45^\circ$. For the majority of cases that have been run including this, the number of projections between 3 to 9 was reliable in the 2-D Hough parameter estimation, and further increase did not significantly improve the estimation performance. As expected, the more image frames used in the time-sequence data the better the parameter estimation accuracy was observed throughout the experiments. More importantly, the algorithm performance was robust in that the tracking ability degrades gracefully with respect to decreasing the signal-to-noise ratio to a low level. The simulation results for the 2-D track map sequence method on the other hand showed a comparable performance to our proposed method down to the SNRs of 15 dB.

Table 1. 2-D parameter estimation of the track with $(\rho = 18, \theta = 45^\circ)$ in HiCamp I.

PROJ	Frame	Estimated 2-D Hough Parameters (ρ, θ)			
		13.2 dB	11.9 dB	8.95 dB	7.75 dB
3	15	(18, 38°)	(18, 38°)	(17, 28°)	(17, 28°)
	20	(18, 45°)	(17, 36°)	(17, 28°)	(22, 67°)
	25	(18, 45°)	(18, 45°)	(18, 45°)	(18, 45°)
6	15	(18, 38°)	(16, 36°)	(23, 72°)	(23, 72°)
	20	(18, 45°)	(17, 36°)	(22, 66°)	(23, 72°)
	25	(18, 45°)	(18, 45°)	(18, 45°)	(18, 45°)
9	15	(18, 38°)	(16, 37°)	(20, 59°)	(23, 78°)
	20	(18, 45°)	(16, 37°)	(20, 59°)	(21, 70°)
	25	(18, 45°)	(18, 45°)	(18, 45°)	(18, 45°)

However, its performance degraded significantly for the SNRs below 13.2 dB. In other words, the 2-D track parameter estimation using the 2-D track map method was no longer robust for the SNRs of 11.9, 8.95, and 7.95 dBs. The entire simulation results show that our algorithm is superior to that of the 2-D track map sequence method. It is also comparable to the results produced by processing the entire set of the original image data as a whole.

Furthermore, many more sets of target trajectories were generated in order to test our algorithm's ability estimating the 3-D locations of moving targets in adverse, noisy conditions. The simulations yielded promising results estimating the 3-D vectors of embedded, dim. moving targets with a good estimation accuracy down to SNR of 8.50 dB. From the simulation results, it became evident that our projection-based method utilizing multiple projection frames performed more robust and superior in comparison to that of using only a 2-D track map. The average number of projections that performs best is experimentally known to us as six to eight in this 3-D directional motion vector estimation. A typical 3-D tracking problem is visualized in Figure 4. When the true 3-D target motion vector is $(1.0, -1.0, 1.0)$ in x , y , and temporal direction, respectively, the figure visualizes the 3-D reconstruction of the 3-D estimated trajectory at the SNR of 11.9 dB. Using six projections taken from

twenty-five frames of the time-sequential HiCamp data, the simulation yielded the 3-D directional motion vector estimate of $(1.00, -0.96, 0.90)$ and the average error distance between the estimated 3-D target track and the true track of less than 0.82 pixel.

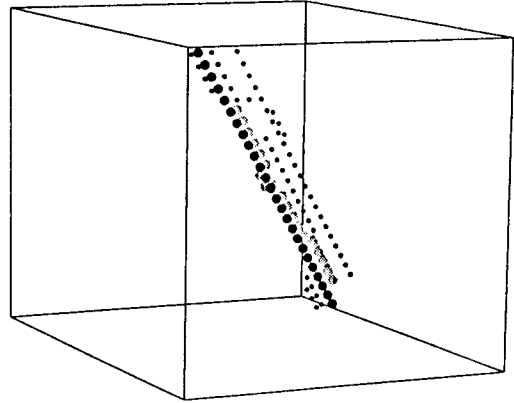


Fig. 4. 3-D reconstruction of the estimated track at SNR of 11.9 dB.

Finally, some multiple target track cases are also simulated. As shown in Figure 5, two 3-D multiple trajectories were estimated and reconstructed through the backward projection at the SNR of 21.2 dB. Ten projection frames were taken from twenty-

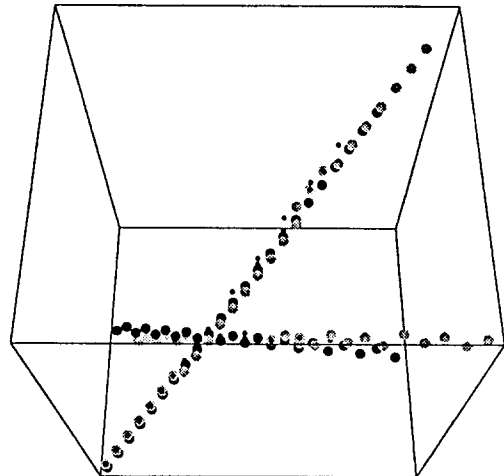


Fig. 5. 3-D multi-target parameter estimation at SNR of 21.2 dB.

three time-sequential data frames. While the true 3-D directional motion vectors were (1.00, 1.00, 1.00) and (1.00, -0.50, 1.00), the found track vector estimates were (1.00, 0.97, 1.05) and (1.00, -0.47, 1.25), respectively.

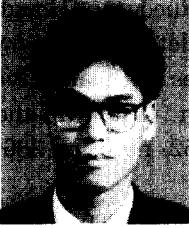
IV. Conclusions

The focus of the paper has been on the 3-D track parameter estimation of small, dim, moving targets embedded in a sequence of digital images. The 3-D modified Radon transform leading into our generalized projection-based transformation method incorporating maximum value projection algorithm was derived. The simulations yielded promising results showing an ability and robustness to detect and estimate the 3-D locations of the embedded, dim, moving targets with a good estimation accuracy at very low SNRs.

References

- [1] N.C. Mohanty, "Computer tracking of moving point targets in space," *IEEE Transactions on Pattern Analysis and Machine Intelligence*, vol.3, pp.606-611, September 1981.
- [2] S.C. Pohlig, "Algorithm for detection of moving optical targets," *IEEE Transactions on Aerospace and Electronic Systems*, vol. AES-25, no.1, pp. 56-62, January 1989.
- [3] J.H. Choi and S.A. Rajala, "Tracking of unresolved targets in infrared imagery using projection-based methods," *Proceedings of SPIE - VCIP' 92*, November 1992.
- [4] A.E. Cowart, W.E. Snyder, and W.H. Ruedger, "The detection of unresolved targets using the Hough transform," *Computer Vision, Graphics, and Image Processing*, vol.21, pp.222-238, 1983.
- [5] M.L. Padgett, S.A. Rajala, W.E. Snyder, and W.H. Ruedger, "Detection of maneuvering target tracks," *Proceedings of SPIE*, vol.575, pp.145-155, August 1985.
- [6] D.J. Hunt, L.W. Nolte, A.R. Reibman, and W.H. Ruedger, "Hough transform and signal detection theory performance for images with additive noise," *Computer Vision, Graphics, and Image Processing*, vol. 52, no.6, pp.386-401, December 1990.
- [7] D.J. Hunt, "The performance of the Hough transform and signal detection theory for the detection and tracking of dim, moving targets," Ph.D. Thesis, Duke University, 1990.
- [8] J. Radon, "Über die bestimmung von funktionen durch ihre interralwerte laenges gewisser mannig faltigkeiten (On the determination of functions from their integrals along certain manifolds)," *Berichte Saechsische Akas. Wissenschaft, Leipzig, Math.-Phys. Klass*, vol.69, pp.262-277, 1917.
- [9] G.R. Gindi and A.F. Gmitro, "Optical feature extraction via the Radon transform," *Optical Engineering*, vol. 23, no.5, pp.499-506, 1984.
- [10] G. Herman, *Image reconstruction from projections - The fundamentals of computerized tomography*, Academic Press, New York, 1980.
- [11] G. Belykin, "Discrete Radon transform," *IEEE Transactions on Acoustics, Speech, and Signal Processing*, vol.35, no.2, pp.162-172, 1987.
- [12] R.M. Lewis, "Physical optics inverse diffraction," *IEEE Trans. Anten. Propagat.*, vol.17, pp.308-314, May 1969.
- [13] Peter L. Chu, "Optimal projection for multidimensional signal detection," *IEEE Transactions on Acoustics, Speech, and Signal Processing*, vol.36, no.5, pp.755-786, May 1988.

— 著 者 紹 介 —



崔在虎(正會員)

1963年 8月 14日生. 1985年 5月
NCSU(노스캐롤라이나 주립대)
전기 및 컴퓨터 공학과 졸업.
1988年 5月 NCSU 전기 및 컴퓨
터 공학과 공학석사. 1993年 5月
NCSU 전기 및 컴퓨터 공학과 컴
퓨터 공학박사. 1990年 1月 ~ 1993年 5月
Research Triangle Institute. R.T.P., N.C.,
U.S.A. 시스템 공학 연구소 연구원. 1994年 3月 ~
현재 전북대학교 컴퓨터 공학과 전임강사. 주관심 분
야는 다차원 신호처리, 영상통신, sensor fusion 등
임.

郭勳星(正會員) 第 31卷 B編 第 1號 參照

현재 전북대학교 컴퓨터 공학과 교수